Production of a neutron-rich ${}^{6}_{\Lambda}$H hypernucleus in the ^{6}Li(π^-, K^+) reaction

Toru Harada[1,2,*] and Yoshiharu Hirabayashi[3]

[1]*Research Center for Physics and Mathematics, Osaka Electro-Communication University, Neyagawa, Osaka, 572-8530, Japan*

[2]*J-PARC Branch, KEK Theory Center, Institute of Particle and Nuclear Studies, High Energy Accelerator Research Organization (KEK), 203-1, Shirakata, Tokai, Ibaraki, 319-1106, Japan*

[3]*Information Initiative Center, Hokkaido University, Sapporo, 060-0811, Japan*

(Received 17 October 2016; revised manuscript received 23 February 2017; published 19 April 2017)

We study phenomenologically the production of the neutron-rich hypernucleus ${}^{6}_{\Lambda}$H in the ^{6}Li(π^-, K^+) reaction at 1.2 GeV/c, using a distorted-wave impulse approximation in a one-step mechanism, $\pi^- p \to K^+\Sigma^-$ via Σ^- doorways caused by $\Sigma^- p \leftrightarrow \Lambda n$ coupling. The production cross section of ${}^{6}_{\Lambda}$H($1^+_{\rm exc.}$) is evaluated by a coupled (^{5}H-Λ) + (^{5}He-Σ^-) model with a spreading potential, in comparison with the data of the missing mass spectrum at the J-PARC E10 experiment. The result indicates that the Σ^- mixing probabilities in ${}^{6}_{\Lambda}$H($1^+_{\rm exc.}$) are $P_{\Sigma^-} <\sim 0.2\%$ both for s_Σ state and for p_Σ state in order to reproduce no significant peak in the Λ production data, so that the cross section of ${}^{6}_{\Lambda}$H is less than on the order of 0.4 nb/sr. The sensitivity of the $\Sigma\Lambda$ coupling and Λ potentials to the near-Λ-threshold spectrum is discussed. The shape and magnitude of the spectrum provide valuable information on the $\Sigma\Lambda$ coupling in the production mechanism and also the nuclear structure of ${}^{6}_{\Lambda}$H($1^+_{\rm exc.}$).

DOI: 10.1103/PhysRevC.95.044610

I. INTRODUCTION

Recently, the J-PARC E10 collaboration [1,2] performed experimental measurements of the double-charge-exchange (DCX) reaction (π^-, K^+) on a ^{6}Li target at $p_{\pi^-} = 1.2$ GeV/c in order to confirm a neutron-rich hypernucleus ${}^{6}_{\Lambda}$H in which an unbound ^{5}H nuclear core with neutron-proton excess ratio $(N - Z)/(N + Z) = 0.6$ is expected to be stable by Λ stabilization or glue [3,4]. No significant peak structure below and near the ${}^{4}_{\Lambda}$H + $2n$ threshold was observed in missing mass spectra with K^+ forward-direction angles of $\theta_{\rm lab} = 2^\circ$–$14^\circ$. This is inconsistent with the observation by the ^{6}Li($K^-_{\rm stop}, \pi^+$) reaction in FINUDA experiments [5] which indicated evidence of ${}^{6}_{\Lambda}$H with a binding energy of $B_\Lambda({}^{6}_{\Lambda}{\rm H}) = 4.5 \pm 1.2$ MeV with respect to the ^{5}H + Λ threshold.

Dalitz and Levi–Setti [3] first discussed the Λ stabilization of the neutron-rich ${}^{6}_{\Lambda}$H hypernucleus with the particle-unstable ^{5}H nuclear core beyond the neutron-drip line. Akaishi and Myint [6] paid attention to ${}^{6}_{\Lambda}$H as a test ground for an attractive three-body ΛNN force caused by the ΛN–ΣN coupling which may be more coherently enhanced in such neutron-excess environments [7,8]. Thus the 0^+ ground state of ${}^{6}_{\Lambda}$H was predicted to have a large binding energy of $B_\Lambda({}^{6}_{\Lambda}{\rm H}) = 5.8$ MeV with respect to the ^{5}H + Λ threshold due to rather large contribution of 1.4 MeV by the coherent $\Lambda\Sigma$ mixing [6]. Gal and Millener [9] showed that recent shell-model calculations including the $\Lambda\Sigma$ coupling give $B_\Lambda({}^{6}_{\Lambda}{\rm H}) = 3.8 \pm 0.2$ MeV which seems to be in good agreement with $B_\Lambda({}^{6}_{\Lambda}{\rm H}) = 4.5 \pm 1.2$ MeV reported in the FINUDA experiments [5,9]. Hiyama *et al.* [10] suggested a less binding energy of $B_\Lambda({}^{6}_{\Lambda}{\rm H}) = 2.47$ MeV corresponding to an unbound state with respect to the ${}^{4}_{\Lambda}$H + $2n$ threshold in $tnn\Lambda$ four-body cluster-model calculations. The value of $B_\Lambda({}^{6}_{\Lambda}{\rm H})$ is often calculated by the Λ-nucleus potential which strongly depends on the structure of the nuclear core as well as ΛN interaction involving the $\Lambda\Sigma$ coupling. Therefore, it is very important to clarify the production and structure of ${}^{6}_{\Lambda}$H which is strongly related to the structure of ^{5}H in nuclear physics.

The DCX (π^-, K^+) reaction is one of the most promising ways of searching for a bound state of the neutron-rich Λ hypernuclei with stabilized effects by Λ added. Indeed, Saha *et al.* [11] performed the first measurement of a significant yield for the ${}^{10}_{\Lambda}$Li hypernucleus in (π^-, K^+) reactions on a ^{10}B target, whereas no clear peak has been observed with the lack of the experimental statistics. The data show that the absolute cross section for ${}^{10}_{\Lambda}$Li at 1.20 GeV/c ($d\sigma/d\Omega \sim 11$ nb/sr) is twice larger than that at 1.05 GeV/c ($d\sigma/d\Omega \sim 6$ nb/sr). This incident-momentum dependence of $d\sigma/d\Omega$ exhibits a trend in the opposite direction for the theoretical prediction by Tretyakova and Lanskoy [12]. This might imply that the one-step mechanism, $\pi^- p \to K^+\Sigma^-$ via Σ^- doorways caused by the $\Sigma^- p \leftrightarrow \Lambda n$ coupling [13] is rather favored over the two-step mechanism, $\pi^- p \to \pi^0 n$ followed by $\pi^0 p \to K^+\Lambda$ (or $\pi^- p \to K^0\Lambda$ followed by $K^0 p \to K^+ n$) in the production of neutron-rich Λ hypernuclear states, as pointed out in Ref. [11].

In this paper, we study phenomenologically the production of the neutron-rich ${}^{6}_{\Lambda}$H hypernuclear states in the ^{6}Li(π^-, K^+) reaction at 1.2 GeV/c. We demonstrate the calculated spectrum near the Λ threshold within a distorted-wave impulse approximation (DWIA) by using a coupled (^{5}H-Λ) + (^{5}He-Σ^-) model with a spreading potential [14]. Comparing the spectrum with the data of the J-PARC E10 experiment [1,2], we discuss the strengths of the $\Sigma\Lambda$ couplings related to the Σ-mixing probabilities and the strengths of the Λ-^{5}H potentials which depend on the structure of the ^{5}H nuclear core in ${}^{6}_{\Lambda}$H.

II. CALCULATIONS

A. Distorted wave impulse approximation

The inclusive K^+ double-differential laboratory cross section of Λ production on a nuclear target in the DCX (π^-, K^+) reaction [15] is calculated by the Green's function method

*harada@osakac.ac.jp

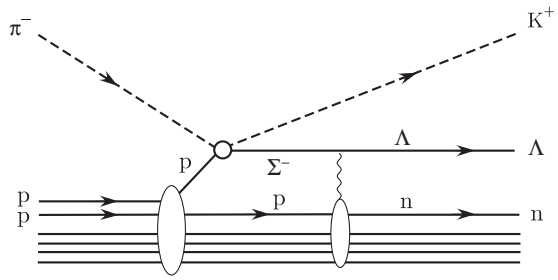

FIG. 1. Diagrams of a one-step mechanism, $\pi^- p \to K^+\Sigma^-$ via Σ^- doorways caused by the $\Sigma^- p \leftrightarrow \Lambda n$ coupling, for production of Λ hypernuclear states by the DCX nuclear (π^-, K^+) reactions.

[16], assuming only the one-step mechanism, $\pi^- p \to K^+\Sigma^-$ via Σ^- doorways caused by the $\Sigma^- p \to \Lambda n$ conversion within the DWIA [13]. Figure 1 illustrates diagrams for the one-step mechanism, $\pi^- p \to K^+\Sigma^-$ via Σ^- doorways in the nuclear (π^-, K^+) reaction. The inclusive K^+ double-differential laboratory cross section on the nuclear target with a spin J_A and its z component M_A [15] is given by

$$\frac{d^2\sigma}{d\Omega dE} = \frac{1}{[J_A]}\sum_{M_A} S(E_B), \tag{1}$$

with $[J_A] = 2J_A + 1$, and the strength function $S(E_B)$ is written by

$$S(E_B) = -\frac{1}{\pi}\mathrm{Im}\sum_{\alpha\alpha'}\int d\boldsymbol{r}d\boldsymbol{r}' F_\Sigma^{\alpha\dagger}(\boldsymbol{r})G_\Sigma^{\alpha\alpha'}(E_B;\boldsymbol{r},\boldsymbol{r}')F_\Sigma^{\alpha'}(\boldsymbol{r}') \tag{2}$$

as a function of the energy E_B for hypernuclear final states, where F_Σ^α is the Σ production amplitude defined by

$$F_\Sigma^\alpha = \beta^{\frac{1}{2}}\overline{f}_{\pi^- p\to K^+\Sigma^-}\chi_{\boldsymbol{p}_K}^{(-)*}\chi_{\boldsymbol{p}_\pi}^{(+)}\langle\alpha|\hat{\psi}_p|\Psi_A\rangle, \tag{3}$$

and $\langle\alpha|\hat{\psi}_p|\Psi_A\rangle$ is a hole-state wave function for a struck proton in the target; α denotes the complete set of eigenstates for the system. The energy and momentum transfer is $\omega = E_K - E_\pi$ and $\boldsymbol{q} = \boldsymbol{p}_K - \boldsymbol{p}_\pi$. The kinematical factor β denotes the translation from a two-body π^--p laboratory system to a π^--^{6}Li laboratory system. $\overline{f}_{\pi^- p\to K^+\Sigma^-}$ is a Fermi-averaged amplitude for the $\pi^- p \to K^+\Sigma^-$ reaction in nuclear medium [17].

Distorted waves for outgoing K^+ and incoming π^- mesons, $\chi_{\boldsymbol{p}_K}^{(-)}$ and $\chi_{\boldsymbol{p}_\pi}^{(+)}$, are estimated with the help of the eikonal approximation in which total cross sections of $\sigma_\pi = 32$ mb for $\pi^- N$ and $\sigma_K = 12$ mb for $K^+ N$, and $\alpha_\pi = \alpha_K = 0$ are used as distortion parameters [17]. The recoil effects are taken into account in our calculations because an effective momentum transfer becomes $q_{\mathrm{eff}} \simeq (1 - 1/A)q \simeq 0.83q$ for the light nuclear system with $A = 6$ due to large momentum transfer $q = 320$–600 MeV/c in the (π^-, K^+) reaction.

Although the 1^+ ground state of ^{6}Li is well described as $\alpha + d$ clusters [18], wave functions for the ^{6}Li target are used in the single-particle (s.p.) description for simplicity. This s.p. description has also been used to study the Σ-nucleus potential for $A = 6$ by the missing-mass ^{6}Li(π^-, K^+) spectrum at the J-PARC E10 experiment [19]. Thus the s.p. wave functions for the proton in $1p_{3/2}$ and $1s_{1/2}$ are calculated by the Woods–Saxon (WS) potential with $a = 0.67$ fm, $R = 1.27A^{1/3} = 2.31$ fm [20]. The strength parameter of the potential is adjusted to be $V_0^N = -55.5$ MeV (-58.0 MeV) for the proton in the $p_{3/2}$ ($s_{1/2}$) state, and $V_{\mathrm{so}}^N = -0.44V_0^N$, in order to reproduce the data of proton s.p. energies in ^{6}Li$(p,2p)$ reactions [21,22]. Thus the s.p. energies for $1p_{3/2}$ and $1s_{1/2}$ amount to -4.61 MeV and -21.48 MeV, respectively. The charge radius for ^{6}Li$(1^+_{\mathrm{g.s.}})$ becomes 2.48 fm of which value is slightly smaller than that of 2.56 ± 0.05 fm in electron elastic scatterings [23] due to the s.p. description. If we replace the s.p. wave function for the $1p_{3/2}$ ($1s_{1/2}$) state by a spectroscopic amplitude describing a $p_{3/2}$ ($s_{1/s}$) proton removal from ^{6}Li$(1^+_{\mathrm{g.s.}})$ within the $\alpha + d$ cluster model [24], we recognize that the calculated cross sections decrease by about 5%, in comparison with the results which will be discussed in Sec. III B. Thus our conclusion obtained in the s.p. description would be reliable.

B. Wave functions for $^6_\Lambda$H

To fully describe the one-step process, as shown in Fig. 1 and to estimate the production cross section of $^6_\Lambda$H, we perform Λ-Σ coupled-channel calculations [14] which reproduce the shape and magnitude of the data of the J-PARC E10 experiment in the Λ and Σ^- quasifree (QF) regions [19]. Here we employ a multichannel coupled wave function of the Λ-Σ nuclear state for a total spin J_B within a weak-coupling basis. It is written as

$$\left|\Psi_{J_B}\left({}^6_Y\mathrm{H}\right)\right\rangle = \sum_{JJ''j_nj_\Lambda}\left[\Phi_{J''}({}^5\mathrm{H}),\varphi_{j_\Lambda}^{(\Lambda)}(\boldsymbol{r}_\Lambda)\right]_{J_B} + \sum_{JJ'j_pj_\Sigma}\left[\Phi_{J'}({}^5\mathrm{He}),\varphi_{j_\Sigma}^{(\Sigma^-)}(\boldsymbol{r}_\Sigma)\right]_{J_B}, \tag{4}$$

with

$$\Phi_{J''}({}^5\mathrm{H}) = \mathcal{A}\left[\Phi_J(s^3p),\varphi_{j_n}^{(n)}(\boldsymbol{r}_n)\right]_{J''}^{({}^5\mathrm{H})},$$
$$\Phi_{J'}({}^5\mathrm{He}) = \mathcal{A}\left[\Phi_J(s^3p),\varphi_{j_p}^{(p)}(\boldsymbol{r}_p)\right]_{J'}^{({}^5\mathrm{He})}, \tag{5}$$

where $\Phi_J(s^3p)$ is a wave function of the s^3p configuration state, $\mathcal{A}$ is the antisymmetrized operator for nucleons, and $\varphi_{j_\Lambda}^{(\Lambda)}$, $\varphi_{j_\Sigma}^{(\Sigma^-)}$, and $\varphi_{j_{n,p}}^{(n,p)}$ describe the relative wave functions of shell model states (that occupy j_Λ, j_Σ, and $j_{n,p}$ orbits) for the Λ, Σ^-, and neutron (proton), respectively; $\boldsymbol{r}_n$ ($\boldsymbol{r}_p$) denotes the relative coordinate between the s^3p nucleus and the neutron or proton, and $\boldsymbol{r}_\Lambda$ ($\boldsymbol{r}_\Sigma$) denotes the relative coordinate between the center of mass of the ^{5}H (^{5}He) subsystem and the Λ (Σ^-). We take the ^{5}H core-nucleus state with $J^\pi = 1/2^+$[ground state (g.s.)], and the ^{5}He core-nucleus states with $J^\pi = 3/2^-$ (g.s.), $1/2^-$, $3/2^+$, and $1/2^+$ that are given in $(1^+ \otimes p_{3/2,1/2}^{-1})_{\frac{3}{2}^-,\frac{1}{2}^-}$ and $(1^+ \otimes s_{1/2}^{-1})_{\frac{3}{2}^+,\frac{1}{2}^+}$ configurations formed by a proton-hole state on ^{6}Li$(1^+_{\mathrm{g.s.}})$. If the Λ component is dominant in a bound or resonant state, we can identify it as a state of the Λ hypernucleus $^6_\Lambda$H, in which the Σ^--mixing probability can be estimated by

$$P_{\Sigma^-} = \sum_{j_\Sigma}\int_0^\infty \rho_{j_\Sigma}(r)r^2dr, \tag{6}$$

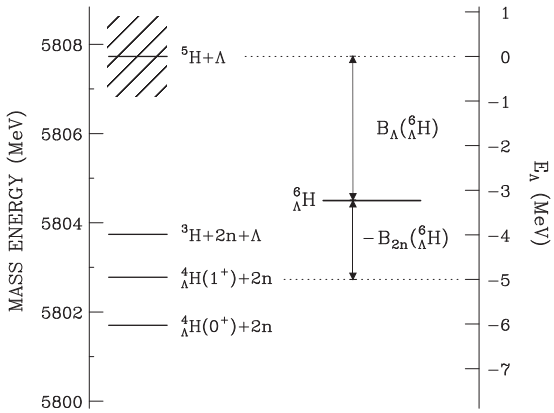

FIG. 2. Energy spectrum and decay threshold of the $^6_\Lambda$H hypernucleus. Binding energies of $B_\Lambda(^6_\Lambda\mathrm{H})$ and $B_{2n}(^6_\Lambda\mathrm{H})$ are defined with respect to $^5\mathrm{H}+\Lambda$ and $^4_\Lambda\mathrm{H}(1^+)+2n$ thresholds, respectively. The threshold-energy difference between $^5\mathrm{H}(1/2^+_{\mathrm{g.s.}})$ and the $^3\mathrm{H}+2n$ threshold is assumed to be 4.0 MeV.

where $\rho_{j_\Sigma}(r)=[\varphi^{(\Sigma^-)}_{j_\Sigma}(r)]^2$ denotes a Σ^- density distribution with the j_Σ shell under the normalization of

$$\sum_{j_\Lambda}\int_0^\infty \rho_{j_\Lambda}(r)r^2dr+\sum_{j_\Sigma}\int_0^\infty \rho_{j_\Sigma}(r)r^2dr=1,$$

together with the Λ density distribution $\rho_{j_\Lambda}(r)$ with j_Λ. Because we assume the Σ^- doorways states that are selectively produced by non-spin-flip processes in the $\pi^-p\to K^+\Sigma^-$ reaction, we consider positive-parity (negative-parity) states with $J^\pi_B=1^+,2^+,3^+,\ldots,$ $(J^\pi_B=0^-,1^-,2^-,3^-,\ldots)$ for final states, which are populated on the nuclear $^6\mathrm{Li}(1^+_{\mathrm{g.s.}})$ targets; the 0^+ ground state of $^6_\Lambda\mathrm{H}(0^+_{\mathrm{g.s.}})$ is forbidden.

Several theoretical calculations [22,25] predicted the ^{5}H ground state with $J^\pi=1/2^+$ (g.s.), $T=3/2$ as a continuum or unbound state, $E_r\simeq 1.6$–3.0 MeV, $\Gamma\simeq 1.5$–4.0 MeV with respect to the $^3\mathrm{H}+2n$ threshold in $^3\mathrm{H}+n+n$ three-body calculations [25] and $E_r\simeq 3.0$–4.5 MeV in standard shell-model calculation with *spsd* space [26,27]. Since the structure of ^{5}H is still uncertain experimentally [10,22,28], we assume that the $^5\mathrm{H}(1/2^+_{\mathrm{g.s.}})$ nuclear core is a resonant state with $E_r=4.0$ MeV [25] in the viewpoint of shell-model calculations, rather than that with $E_r=1.7$ MeV in Ref. [29]. Thus the energy difference between $^5\mathrm{He}+\Sigma^-$ and $^5\mathrm{H}+\Lambda$ channels is $\Delta M=M(^5\mathrm{He})+m_{\Sigma^-}-M(^5\mathrm{H})-m_\Lambda=57.6$ MeV, where $M(^5\mathrm{He})$, $M(^5\mathrm{H})$, m_{Σ^-}, and m_Λ are masses of ^{5}He, ^{5}H, Σ^- and Λ, respectively. Figure 2 illustrates the energy spectrum and decay threshold for the $^6_\Lambda$H hypernucleus, where $B_\Lambda(^6_\Lambda\mathrm{H})$ and $B_{2n}(^6_\Lambda\mathrm{H})$ denote the binding energies with respect to $^5\mathrm{H}+\Lambda$ and $^4_\Lambda\mathrm{H}(1^+)+2n$ thresholds, respectively.

C. Multichannel Green's functions

The Green's function method is one of the most powerful treatments in calculations for the spectrum [16]. The complete Green's function $\boldsymbol{G}(E)$ describes all information concerning $(^5\mathrm{H}\otimes\Lambda)+(^5\mathrm{He}\otimes\Sigma^-)$ coupled-channel dynamics. We obtain it by solving the following equation with the hyperon-nucleus potential $\boldsymbol{U}$ numerically:

$$\boldsymbol{G}(E)=\boldsymbol{G}^{(0)}(E)+\boldsymbol{G}^{(0)}(E)\boldsymbol{U}\boldsymbol{G}(E), \tag{7}$$

where

$$\boldsymbol{G}(E)=\begin{pmatrix}G_\Lambda(E) & G_X(E)\\ G_X(E) & G_\Sigma(E)\end{pmatrix},\quad \boldsymbol{U}=\begin{pmatrix}U_\Lambda & U_X\\ U_X & U_\Sigma\end{pmatrix}, \tag{8}$$

and the free Green's function $\boldsymbol{G}^{(0)}(E)$. The diagonal parts U_Λ (U_Σ) for $\boldsymbol{U}$ are the Λ-nucleus (Σ-nucleus) potentials, and the off-diagonal parts U_X are the $\Sigma\Lambda$ coupling potentials. Thus the inclusive Λ spectrum in Eq. (2) can be decomposed into different physical processes [14,16] by using the identity

$$\begin{aligned}\mathrm{Im}(F^\dagger_\Sigma G_\Sigma(E)F_\Sigma)=&\ F^\dagger_\Sigma\Omega^{(-)\dagger}\big(\mathrm{Im}G^{(0)}_\Lambda(E)\big)\Omega^{(-)}F_\Sigma\\ &+F^\dagger_\Sigma G^\dagger_X(E)(\mathrm{Im}U_\Lambda)G_X(E)F_\Sigma\\ &+F^\dagger_\Sigma G^\dagger_\Sigma(E)(\mathrm{Im}U_\Sigma)G_\Sigma(E)F_\Sigma,\end{aligned} \tag{9}$$

where $\Omega^{(-)}$ is the Möller wave operator and F_Σ is the production amplitude for Σ^-. The remarkable production of $^6_\Lambda$H arises from the term of $F^\dagger_\Sigma G^\dagger_X(\mathrm{Im}U_\Lambda)G_XF_\Sigma$.

The Y-nucleus (optical) potentials for $Y=\Lambda$ or Σ^- are given by the Woods–Saxon (WS) form:

$$U_Y(r)=[V_Y+iW_Yg(E_\Lambda)]f_Y(r), \tag{10}$$

where $f_Y(r)=\{1+\exp[(r-R)/a]\}^{-1}$. For the ^{5}H-$\Lambda$ channel, we use $a=0.60$ fm, $r_0=1.080+0.395A^{-2/3}$ fm and $R=r_0A^{1/3}_{\mathrm{core}}=2.05$ fm [30]. Considering that the ^{5}H nuclear core may be an unbound state or a broad resonant state [10], the strength parameters of V_Λ should be adjusted appropriately to reproduce the experimental data. The spreading imaginary potential, $\mathrm{Im}\,U_Y$, can represent complicated excited states for $^6_\Lambda\mathrm{H}^*$; $g(E_\Lambda)$ is assumed to be an energy-dependent function which linearly increases from 0 at $E_\Lambda=0$ MeV to 1 at $E_\Lambda=60$ MeV with respect to the $^5\mathrm{H}+\Lambda$ threshold, as often used in nuclear optical models. For the ^{5}He-Σ^- potential, we use the WS potential with $R=1.1A^{1/3}_{\mathrm{core}}=1.88$ fm and $a=0.67$ fm, in comparison with the data of the J-PARC E10 experiment [2]. We take the strengths of $(V_\Sigma,W_\Sigma)=(+20\text{ MeV},-20\text{ MeV})$ which can fully reproduce the data in Σ^- region, leading to the reduced χ^2 value of $\chi^2/N\simeq 0.97$ [19]. The spreading potential W_Σ expresses nuclear core breakup processes caused by the $\Sigma^-p\to\Lambda n$ conversion in the ^{5}He nucleus, and its effect is not involved in U_X which we will mention below.

D. $\Sigma\Lambda$ coupling potentials

The $\Sigma\Lambda$ coupling potential U_X in off-diagonal parts of $\boldsymbol{U}$ can be obtained by a two-body ΣN–ΛN potential $v^S_{\Sigma N,\Lambda N}(\boldsymbol{r}',\boldsymbol{r})$ with the spin $S=1$, 0 isospin $I=1/2$ state. Here we use a zero-range interaction $v^S_{\Sigma N,\Lambda N}(\boldsymbol{r}',\boldsymbol{r})=\tilde{v}^S_{\Sigma N,\Lambda N}\delta(\boldsymbol{r}'-\boldsymbol{r})$ in a real potential for simplicity, where $\tilde{v}^S_{\Sigma N,\Lambda N}$ is the strength parameter that should be connected with volume integral $\int v^S_{\Sigma N,\Lambda N}(\boldsymbol{r})d\boldsymbol{r}=\tilde{v}^S_{\Sigma N,\Lambda N}$. Thus the matrix elements can be easily estimated by use of Racah

algebra [31,32]:

$$\begin{aligned} U_X(r) &= \langle [\Phi_{J'}(^5\mathrm{He}) \otimes \mathcal{Y}^{(\Sigma^-)}_{j'\ell's'}(\hat{\boldsymbol{r}})]_{J_B} | \\ &\quad \times \frac{1}{\sqrt{3}} \sum_i v^S_{\Sigma N,\Lambda N}(\boldsymbol{r}'_i,\boldsymbol{r}) \boldsymbol{\tau}_j \cdot \boldsymbol{\phi} \\ &\quad \times | [\Phi_{J'}(^5\mathrm{H}) \otimes \mathcal{Y}^{(\Lambda)}_{j\ell s}(\hat{\boldsymbol{r}})]_{J_B} \rangle \\ &= \sum_{LSK} \tilde{v}^S_{\Sigma N,\Lambda N} C^{J_B}_{LSK}(J'J'') \mathcal{F}^{J'J''}_{LSK}(r), \end{aligned} \tag{11}$$

where $\boldsymbol{\tau}_j$ denotes the jth nucleon isospin operator and $\boldsymbol{\phi}$ is defined as $|\Sigma\rangle = \boldsymbol{\phi}|\Lambda\rangle$ in isospin space [33], and $\mathcal{Y}_{j\ell s} = [Y_\ell \otimes X_{\frac{1}{2}}]_j$ is a spin-orbit function and $C^{J_B}_{LSK}(J'J'')$ is a purely geometrical factor [31]; $\mathcal{F}^{J'J''}_{LSK}(r)$ is the nuclear form factor including a one-body transition density for the $A = 5$ shell model [26] and the center-of-mass correction of a factor $\sqrt{A/(A-1)}$ [34].

Three parameters, $\tilde{v}^1_{\Sigma N,\Lambda N}$, $\tilde{v}^0_{\Sigma N,\Lambda N}$, and V_Λ, are very important for determining the Σ^--mixing probability in ${}^6_\Lambda$H and the production cross section of ${}^6_\Lambda$H within the one-step mechanism [13]. These parameters are strongly connected each other for the shape of the spectrum and its magnitude. The effects of the ΣN–ΛN coupling can be evaluated by the volume integrals for ΣN–ΛN g matrices based on Nijmegen potentials [35–38], in which these values are model dependent; for example, −216.3, −351.0, −478.3, and −826.6 MeV fm^3 for $S = 1$ in ESC08c, ESC08a, ESC08b, and ESC08a″ potentials with $k_F = 1.0$ fm^{-1}, respectively [38]. Here we use the volume integrals calculated by the g matrix based on the D2′ potential (D2′g) which can reproduce the binding energies of ${}^3_\Lambda$H, ${}^4_\Lambda$He, ${}^4_\Lambda$He*, and ${}^5_\Lambda$He [39], and we assume $\tilde{v}^1_{\Sigma N,\Lambda N} = -900$ MeV ($\tilde{v}^0_{\Sigma N,\Lambda N} = 500$ MeV) as a standard, which corresponds to $\tilde{v}^1_{\Sigma N,\Lambda N} = -941.2$ MeV ($\tilde{v}^0_{\Sigma N,\Lambda N} = 513.6$ MeV) obtained by D2′g with $k_F = 1.05$ fm^{-1}. To see the dependence of the spectrum on the ΣN–ΛN coupling strength, we choose typical values of $\tilde{v}^1_{\Sigma N,\Lambda N} = -450$, −900, −1350, and −1800 MeV ($\tilde{v}^0_{\Sigma N,\Lambda N} = 250$, 500, 750, and 1000 MeV). Thus we attempt to determine important parameters of $\tilde{v}^S_{\Sigma N,\Lambda N}$ and V_Λ, demonstrating the calculated spectrum in comparison with the shape and magnitude of the experimental data, whereas no significant peak structure was observed near the ${}^4_\Lambda$H + $2n$ threshold in the J-PARC E10 experiment.

III. RESULTS

Now let us examine the dependence of the shape and magnitude of the spectrum on $\tilde{v}^S_{\Sigma N,\Lambda N}$ and V_Λ, comparing the calculated inclusive Λ spectrum for ${}^6_\Lambda$H with the data of the ^{6}Li(π^-, K^+) reaction at the J-PARC E10 experiment. In our calculation, we also took the energy-dependent Fermi-averaged t matrix for the $\pi^- p \to K^+\Sigma^-$ reaction which is essential to explain the Σ^- QF spectra of the (π^-, K^+) data on nuclear targets [17]. Therefore, it should be noticed that the following calculated spectra have reproduced the data in the Σ^- and Λ QF regions [19].

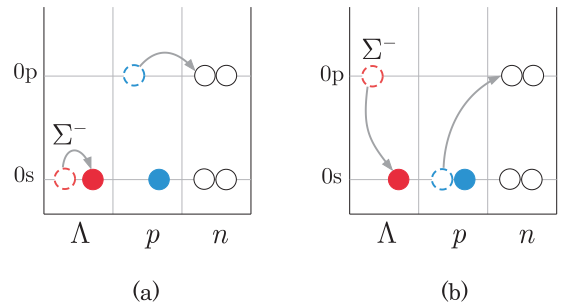

FIG. 3. Schematic illustration of shell-model configurations for (a) $p_p s_{\Sigma^-} \to p_n s_\Lambda$ transitions from $s_p^{-1} s_\Sigma$ components, and (b) $s_p p_{\Sigma^-} \to p_n s_\Lambda$ transitions from $p_p^{-1} p_\Sigma$ components in ${}^6_\Lambda$H($1^+_{\mathrm{exc.}}$).

A. Σ^- doorways

The nuclear (π^-, K^+) reaction can predominantly populate spin-stretched states of ^{5}He $\otimes\, \Sigma^-$ doorways with $T = 3/2$ because the momentum transfer is very large ($q \simeq 359$ MeV/c around the Λ threshold) in the $\pi^- p \to K^+\Sigma^-$ reaction at 1.20 GeV/c [40]. It is also considered that non-spin-flip processes are dominant near the forward direction in this reaction [41]. Thus the 0^+ ground state of ${}^6_\Lambda$H($0^+_{\mathrm{g.s.}}$) that is expected to have a large contribution by the coherent $\Lambda\Sigma$ mixing [6] is forbidden by spin-parity conservation when choosing ^{6}Li($1^+_{\mathrm{g.s.}}$) as a target, whereas the 1^+ excited state of ${}^6_\Lambda$H($1^+_{\mathrm{exc.}}$) can be produced in the reaction. For ${}^6_\Lambda$H($1^+_{\mathrm{exc.}}$) in the one-step mechanism via Σ^- doorways, we have

$$\begin{aligned} &{}^6\mathrm{Li}(1^+_{\mathrm{g.s.}}; T = 0) \\ &\xrightarrow[\Delta L=0]{s_p \to s_\Sigma} [{}^5\mathrm{He}(3/2^+_{\mathrm{exc.}}, 1/2^+_{\mathrm{exc.}}; T_c = 1/2) \otimes (s_{1/2})_{\Sigma^-}]_{1^+} \\ &\rightleftarrows [{}^5\mathrm{H}(1/2^+_{\mathrm{g.s.}}; T_c = 3/2) \otimes (s_{1/2})_\Lambda]_{1^+} \end{aligned} \tag{12}$$

in the $s_p^{-1} s_\Sigma$ configuration formed by the $\pi^- p \to K^+\Sigma^-$ reaction, and

$$\begin{aligned} &{}^6\mathrm{Li}(1^+_{\mathrm{g.s.}}; T = 0) \\ &\xrightarrow[\Delta L=0,2]{p_p \to p_\Sigma} [{}^5\mathrm{He}(3/2^-_{\mathrm{g.s.}}, 1/2^-_{\mathrm{exc.}}; T_c = 1/2) \otimes (p_{3/2,1/2})_{\Sigma^-}]_{1^+} \\ &\rightleftarrows [{}^5\mathrm{H}(1/2^+_{\mathrm{g.s.}}; T_c = 3/2) \otimes (s_{1/2})_\Lambda]_{1^+} \end{aligned} \tag{13}$$

in the $p_p^{-1} p_\Sigma$ configuration. Figure 3 illustrates these shell-model configurations in ${}^6_\Lambda$H($1^+_{\mathrm{exc.}}$) schematically. The former process indicates the coherent $\Lambda\Sigma$ coupling with the $p_p s_{\Sigma^-} \to p_n s_\Lambda$ transition [7]. The latter process also contributes to ${}^6_\Lambda$H($1^+_{\mathrm{exc.}}$) due to the $s_p p_{\Sigma^-} \to p_n s_\Lambda$ transition which induces nucleon-hole states with nuclear core-excitation in the Λ hypernucleus, as discussed in *ab initio* calculations for ${}^5_\Lambda$He($1/2^+_{\mathrm{g.s.}}$) by Nemura *et al.* [42]. The type of this coupling is called as "incoherent" $\Lambda\Sigma$ coupling. We used single-particle wave functions for a proton in ^{6}Li($1^+_{\mathrm{g.s.}}$), reproducing the s-hole and p-hole energies in ^{6}Li(p, $2p$) reactions [21].

B. ${}^6_\Lambda$H(1^+_{exc})

Let us consider the $\Sigma\Lambda$ coupling potentials which determine the Σ^- mixing probabilities related to the production

TABLE I. Configurations for ${}^{6}_{\Lambda}\mathrm{H}(1^{+}_{\mathrm{exc.}})$.

${}^{5}\mathrm{H}(T=3/2)\otimes\Lambda$		${}^{5}\mathrm{He}(T=1/2)\otimes\Sigma^{-}$	
J^{π}_{C}	$(\ell j)_{\Lambda}$	J^{π}_{C}	$(\ell j)_{\Sigma^-}$
$1/2^{+}$	$s_{1/2}$	$3/2^{-}, 1/2^{-}$	$p_{3/2}, p_{1/2}, f_{5/2}$
		$1/2^{+}, 3/2^{+}$	$s_{1/2}, d_{5/2}, d_{3/2}$

cross section for ${}^{6}_{\Lambda}\mathrm{H}(1^{+}_{\mathrm{exc.}})$ in one-step mechanism. In Table I, we show configurations of the $[J^{\pi}_{C}\otimes(\ell j)_{Y}]_{1^+}$ state in ${}^{6}_{\Lambda}\mathrm{H}(1^{+}_{\mathrm{exc.}})$ composed by the $A=5$ core nucleus with J^{π}_{C} and (ℓj)-shell hyperon. In Fig. 4, we display the calculated $\Sigma\Lambda$ coupling potentials $U_X(r)$ between $[{}^{5}\mathrm{He}(J^{\pi}_{C})\otimes(\ell j)_{\Sigma^-}]$ and $[{}^{5}\mathrm{H}(1/2^{+}_{\mathrm{g.s.}})\otimes(s_{1/2})_{\Lambda}]$ states in ${}^{6}_{\Lambda}\mathrm{H}(1^{+}_{\mathrm{exc.}})$ as a function of a relative distance between ^{5}H (^{5}He) and $Y=\Lambda$ (Σ^-), using the $\Sigma\Lambda$ coupling strengths of $\tilde{v}^{1}_{\Sigma N,\Lambda N}=-900$ MeV and $\tilde{v}^{0}_{\Sigma N,\Lambda N}=500$ MeV in Eq. (11); these coupling potentials are classified by the orbital angular momentum transfers $\Delta\ell$ to the hyperon in ${}^{6}_{\Lambda}\mathrm{H}(1^{+}_{\mathrm{exc.}})$, where $\Delta\ell=|\ell_{\Sigma^-}-\ell_{\Lambda}|$. We find that the following coupling potentials are dominant:

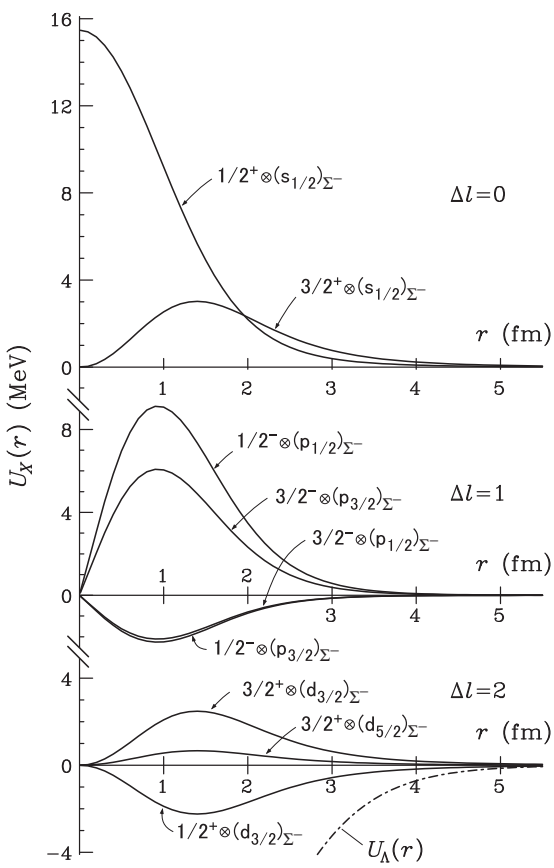

FIG. 4. Calculated $\Sigma\Lambda$ coupling potentials $U_X(r)$ between $[{}^{5}\mathrm{He}(J^{\pi}_{C})\otimes(\ell j)_{\Sigma^-}]$ and $[{}^{5}\mathrm{H}(1/2^{+}_{\mathrm{g.s.}})\otimes(s_{1/2})_{\Lambda}]$ with $\Delta\ell=|\ell_{\Sigma^-}-\ell_{\Lambda}|=0,1,2$ in ${}^{6}_{\Lambda}\mathrm{H}(1^{+}_{\mathrm{exc.}})$ at $E_{\Lambda}=0$ MeV in Eq. (11), as a function of the relative distance between ^{5}H (^{5}He) and Λ (Σ^-). $\tilde{v}^{1}_{\Sigma N,\Lambda N}=-900$ MeV and $\tilde{v}^{0}_{\Sigma N,\Lambda N}=500$ MeV are used. The dot-dashed curve denote the ^{5}H-Λ potential as a guide.

i. $[1/2^{+}\otimes(s_{1/2})_{\Sigma^-}]$–$[1/2^{+}\otimes(s_{1/2})_{\Lambda}]$ for $\Delta\ell=0$;
ii. $[1/2^{-}\otimes(p_{1/2})_{\Sigma^-}]$–$[1/2^{+}\otimes(s_{1/2})_{\Lambda}]$ for $\Delta\ell=1$;
iii. $[3/2^{-}\otimes(p_{3/2})_{\Sigma^-}]$–$[1/2^{+}\otimes(s_{1/2})_{\Lambda}]$ for $\Delta\ell=1$.

This nature may originate from the fact that a significant $\pi+\rho$ meson exchange related with the SU(3) coupling constant generates a $(\boldsymbol{\sigma}_N\cdot\boldsymbol{\sigma}_Y)(\boldsymbol{\tau}_N\cdot\boldsymbol{\phi}_Y)$ component in ΛN–ΣN potentials, and that the nuclear form factors $\mathcal{F}^{J'J''}_{LSK}(r)$ in Eq. (11) have the collectivity of nuclear core excitations in microscopic $A=5$ shell-model calculations. We recognize that the $s_p p_{\Sigma^-}\to p_n s_{\Lambda}$ transitions are significant to describe Λ-Σ dynamics in ${}^{6}_{\Lambda}\mathrm{H}(1^{+}_{\mathrm{exc.}})$ as well as the $p_p s_{\Sigma^-}\to p_n s_{\Lambda}$ transitions caused by coherent $\Lambda\Sigma$ couplings, as discussed by Akaishi *et al.* [7].

To see the dependence of the spectrum on $\tilde{v}^{S}_{\Sigma N,\Lambda N}$, here we take $V_{\Lambda}=-19$ MeV for ${}^{6}_{\Lambda}\mathrm{H}(1^{+}_{\mathrm{exc.}})$, whose potential gives the binding energy of $B_{\Lambda}({}^{6}_{\Lambda}\mathrm{H})=1.492$ MeV when omitting $\tilde{v}^{S}_{\Sigma N,\Lambda N}$. This value of B_{Λ} is moderately larger than that of $B_{\Lambda}({}^{4}_{\Lambda}\mathrm{H})=0.96\pm0.04$ MeV for the ${}^{4}_{\Lambda}\mathrm{H}(1^{+})$ subsystem in ${}^{6}_{\Lambda}$H. We consider single-particle wave functions for Λ, n in ${}^{6}_{\Lambda}\mathrm{H}(1^{+}_{\mathrm{exc.}})$ as well as those for ${}^{6}_{\Lambda}\mathrm{H}(0^{+}_{\mathrm{g.s.}})$ in which the s_{Λ} state has the root-mean-square radius of $\langle r^2\rangle^{1/2}=3.35$ fm, in comparison with $\langle r^2\rangle^{1/2}=4.01$ fm for valence neutrons in ${}^{6}_{\Lambda}$H. Thus the Λ, n distributions in ${}^{6}_{\Lambda}$H simulate a similar structure to the layer distributions of single-particle t, Λ, and n densities obtained by the $tnn\Lambda$ four-body calculations [10].

1. Binding energies and Σ^--mixing probabilities

In Table II, we show the results of the binding energies and Σ^--mixing probabilities in ${}^{6}_{\Lambda}\mathrm{H}(1^{+}_{\mathrm{exc.}})$. When we take $\tilde{v}^{1}_{\Sigma N,\Lambda N}=-450$, -900, -1350, and -1800 MeV ($\tilde{v}^{0}_{\Sigma N,\Lambda N}=250$, 500, 750, and 1000 MeV), we find the Σ^- mixing probabilities of $P_{\Sigma^-}=0.07\%$, 0.32%, 0.79%, and 1.58%, respectively. We stress that there appear not only s_{Σ} components but also p_{Σ} components in the Σ^--mixing probabilities; the value of $P_{\Sigma^-}(p_{\Sigma})=0.04\%$–$0.82\%$ is larger than that of $P_{\Sigma^-}(s_{\Sigma})=0.03\%$–$0.68\%$. The d_{Σ} components are relatively small. The corresponding energy positions of ${}^{6}_{\Lambda}\mathrm{H}(1^{+}_{\mathrm{exc.}})$ are shifted downward by the $\Sigma\Lambda$ coupling. We obtain the energy-level shift ΔE_{Λ} caused by the $p_p s_{\Sigma^-}\leftrightarrow p_n s_{\Lambda}$ coupling in Eq. (12), e.g., $\Delta E_{\Lambda}\simeq-148$ keV when $\tilde{v}^{1}_{\Sigma N,\Lambda N}=-900$ MeV and $\tilde{v}^{0}_{\Sigma N,\Lambda N}=500$ MeV. This value is slightly smaller than that of ${}^{9,10}_{\Lambda}$Li in several microscopic shell-model calculations [43,44]. For ΔE_{Λ} caused by the $s_p p_{\Sigma^-}\leftrightarrow p_n s_{\Lambda}$ coupling in Eq. (13), we estimate $\Delta E_{\Lambda}\simeq-201$ keV. This effect may be often eliminated in the model space by g-matrix description, and it is not taken into account explicitly in standard calculations [43,44].

In Fig. 5, we display the density distribution of $\rho_{\alpha_Y}(r)$ for $Y=\Lambda,\Sigma^-$ with $\alpha=\{n\ell j\}$ in ${}^{6}_{\Lambda}\mathrm{H}(1^{+}_{\mathrm{exc.}})$ when we use the $\Sigma\Lambda$ coupling potential given in Fig. 4. Thus we have $P_{\Sigma^-}(s_{\Sigma})=0.13\%$ and $P_{\Sigma^-}(p_{\Sigma})=0.17\%$, as seen in Table II. We find that the Σ^- components are located near the center of ${}^{6}_{\Lambda}\mathrm{H}(1^{+}_{\mathrm{exc.}})$, e.g., the renormalized root-mean-square radius of $\langle r^2\rangle^{1/2}=1.47$ (1.70) fm for s_{Σ} (p_{Σ}) states, respectively, in comparison with those of $\langle r^2\rangle^{1/2}=1.98$ (3.03) fm for s_p (p_p) states in ^{6}Li$(1^{+}_{\mathrm{g.s.}})$. This compactness of these Σ^- distributions

TABLE II. Calculated production cross sections of $d\sigma/d\Omega$ for ${}^{6}_{\Lambda}\mathrm{H}(1^{+}_{\mathrm{exc.}})$ by one-step mechanism in the ${}^{6}\mathrm{Li}(\pi^{-}, K^{+})$ reaction at 1.2 GeV/c (7°), depending on the $\Sigma\Lambda$ coupling parameters of $\tilde{v}^{S}_{\Sigma N,\Lambda N}$. P_{Σ^-} is the Σ^--mixing probability, and $B_{\Lambda}({}^{6}_{\Lambda}\mathrm{H})$ and $B_{2n}({}^{6}_{\Lambda}\mathrm{H})$ are binding energies of Λ and $2n$, respectively. $V_{\Lambda} = -19$ MeV is used.

$\tilde{v}^{S}_{\Sigma N,\Lambda N}$ (MeV)		$B_{\Lambda}({}^{6}_{\Lambda}\mathrm{H})$	$B_{2n}({}^{6}_{\Lambda}\mathrm{H})$	P_{Σ^-} (%)				$d\sigma/d\Omega$ (nb/sr)		
$S=1$	$S=0$	(MeV)	(MeV)	s_{Σ}	p_{Σ}	d_{Σ}	Total	s_p^{-1}	p_p^{-1}	Total
0	0	1.492	−3.508	0.00	0.00	0.00	0.00	0.00	0.00	0.00
−450	250	1.576	−3.424	0.03	0.04	0.00	0.07	0.03	0.01	0.04
−900	500	1.841	−3.159	0.13	0.17	0.02	0.32	0.16	0.06	0.22
−1350	750	2.328	−2.672	0.34	0.41	0.04	0.79	0.44	0.15	0.59
−1800	1000	3.100	−1.900	0.68	0.82	0.08	1.58	1.00	0.32	1.32

may originate from the short-range nature of the $\Sigma\Lambda$ coupling potentials obtained in Eq. (11), and this nature is already seen in the *ab initio* calculation by Ref. [42].

2. *Inclusive Λ spectra and cross sections*

In Fig. 6, we show the calculated inclusive Λ spectrum of the ${}^{6}\mathrm{Li}(\pi^-, K^+)$ reaction at $p_{\pi^-} = 1.20$ GeV/c and $\theta_{\mathrm{lab}} = 7°$, together with the data for the average cross section $\bar{\sigma}_{2°-14°}$, taken into account a detector resolution of 3.2 MeV FWHM. We find that the calculated spectrum below the ${}^{5}\mathrm{H} + \Lambda$ threshold is rather sensitive to $\tilde{v}^{S}_{\Sigma N,\Lambda N}$ in the one-step mechanism, where ${}^{6}_{\Lambda}\mathrm{H}(1^{+}_{\mathrm{exc.}})$ is particle unstable above the ${}^{4}_{\Lambda}\mathrm{H} + 2n$ threshold. The integrated cross sections for ${}^{6}_{\Lambda}\mathrm{H}(1^{+}_{\mathrm{exc.}})$ account for $d\sigma/d\Omega = 0.04$–1.32 nb/sr for $\tilde{v}^{1}_{\Sigma N,\Lambda N} = (-450)$–$(-1800)$ MeV and $\tilde{v}^{0}_{\Sigma N,\Lambda N} = 250$–$1000$ MeV, as listed in Table II. We display the values of $d\sigma/d\Omega$ for ${}^{6}_{\Lambda}\mathrm{H}(1^{+}_{\mathrm{exc.}})$ as a bin with a finite width of 1 MeV for particle decay channels at $M_{\mathrm{x}} \simeq 5806.16$–$5804.63$ MeV/c^2, as also shown in Fig. 6. It is remarkable that the Λ production spectra are composed of proton-hole states, s_p^{-1} and p_p^{-1}, populated by the (π^-, K^+) reactions. The value of $d\sigma(p_p^{-1})/d\Omega = 0.01$–$0.32$ nb/sr is considerably smaller than that of $d\sigma(s_p^{-1})/d\Omega = 0.03$–$1.00$ nb/sr, whereas $P_{\Sigma^-}(p_{\Sigma}) = 0.04\%$–$0.82\%$ is larger than $P_{\Sigma^-}(s_{\Sigma}) = 0.03\%$–$0.68\%$, as mentioned above.

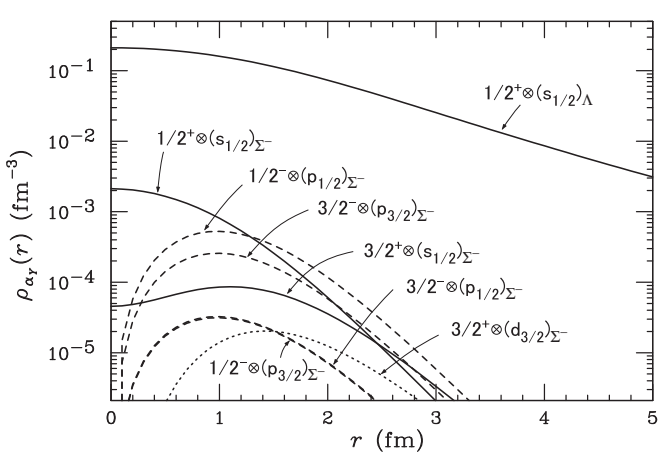

FIG. 5. Single-particle density distributions of Λ and Σ^- in ${}^{6}_{\Lambda}\mathrm{H}(1^{+}_{\mathrm{exc.}})$, $\rho_{\alpha_Y}(r)$ with $\alpha = \{n\ell j\}$ and $Y = \Lambda, \Sigma^-$, as a function of the relative distance between ${}^{5}\mathrm{H}$ (${}^{5}\mathrm{He}$) and Λ (Σ^-). The $\Sigma\Lambda$ coupling potentials given in Fig. 4 are used. Solid, dashed, and dotted curves denote the components of the hyperon densities in $(s_{1/2})_Y$, $(p_{3/2,1/2})_Y$, and $(d_{5/2})_Y$ orbits, respectively.

IV. DISCUSSION

A. *s*-hole proton vs *p*-hole proton

To see the feasibility of producing the neutron-rich Λ hypernucleus in the one-step mechanism, we consider the contribution of the inclusive spectra via Σ^- doorways from the proton p^{-1} (s^{-1}) state on the ${}^{6}\mathrm{Li}$ target. The integrated laboratory cross section may be roughly written as

$$\frac{d\sigma(j_p^{-1})}{d\Omega_L} \approx \beta|\bar{f}_{\pi^- p\to K^+\Sigma^-}|^2 \times S_p(j_p)|F^{(j_p\to j_{\Sigma})}_{\Delta L}(q)|^2 P_{\Sigma^-}(j_{\Sigma}), \quad (14)$$

where $S_p(j_p)$ is a spectroscopic factor for j_p-shell proton, and $\bar{f}_{\pi^- p\to K^+\Sigma^-}$ is a Fermi-averaged amplitude for the $\pi^- p \to K^+\Sigma^-$ reactions. Thus we recognize the behavior of the form factor $F^{(j_p\to j_{\Sigma})}_{\Delta L}(q)$ for the $j_p \to j_{\Sigma}$ transition with angular-momentum transfer ΔL, depending on the momentum transfer q in the (π^-, K^+) reactions. Using a harmonic-oscillator model in the plane-wave approximation [40], we can estimate

$$\frac{S_p(p_p)|F^{(p_p\to p_{\Sigma})}_{\Delta L=0,2}(q)|^2}{S_p(s_p)|F^{(s_p\to s_{\Sigma})}_{\Delta L=0}(q)|^2} \approx \frac{1}{2}\left[1 - \frac{1}{3}(\tilde{b}q)^2 + \frac{7}{180}(\tilde{b}q)^4\right] \simeq 0.20 \quad (15)$$

for $q \simeq 360$ MeV/c corresponding to the Λ threshold at 1.2 GeV/c. Here we adopted $S_p(p_p)/S_p(s_p) \simeq 1/2$ for ${}^{6}\mathrm{Li}$ and the oscillator radius parameter $\tilde{b} = 1.38$ fm. This $\tilde{b}$ value indicates that the Σ^- components are distributed near the center of ${}^{6}_{\Lambda}\mathrm{H}(1^{+}_{\mathrm{exc.}})$. As a result, we confirm that the value of $d\sigma(p_p^{-1})/d\Omega$ is considerably smaller than that of $d\sigma(s_p^{-1})/d\Omega$, whereas $P_{\Sigma^-}(p_{\Sigma})$ and $P_{\Sigma^-}(s_{\Sigma})$ have almost the same value.

B. $\tilde{v}^{S}_{\Sigma N,\Lambda N}$ strengths

As far as $\tilde{v}^{1}_{\Sigma N,\Lambda N} = (0.0)$–$(-900)$ MeV and $\tilde{v}^{0}_{\Sigma N,\Lambda N} = 0.0$–$500$ MeV leading to $P_{\Sigma^-}(s_{\Sigma}) = 0.0\%$–$0.13\%$ and $P_{\Sigma^-}(p_{\Sigma}) = 0.0\%$–$0.17\%$, therefore, the calculated spectra can fairly explain the data of the J-PARC E10 experiment. No peak structure of ${}^{6}_{\Lambda}\mathrm{H}$ originates from the small $\Sigma\Lambda$ coupling

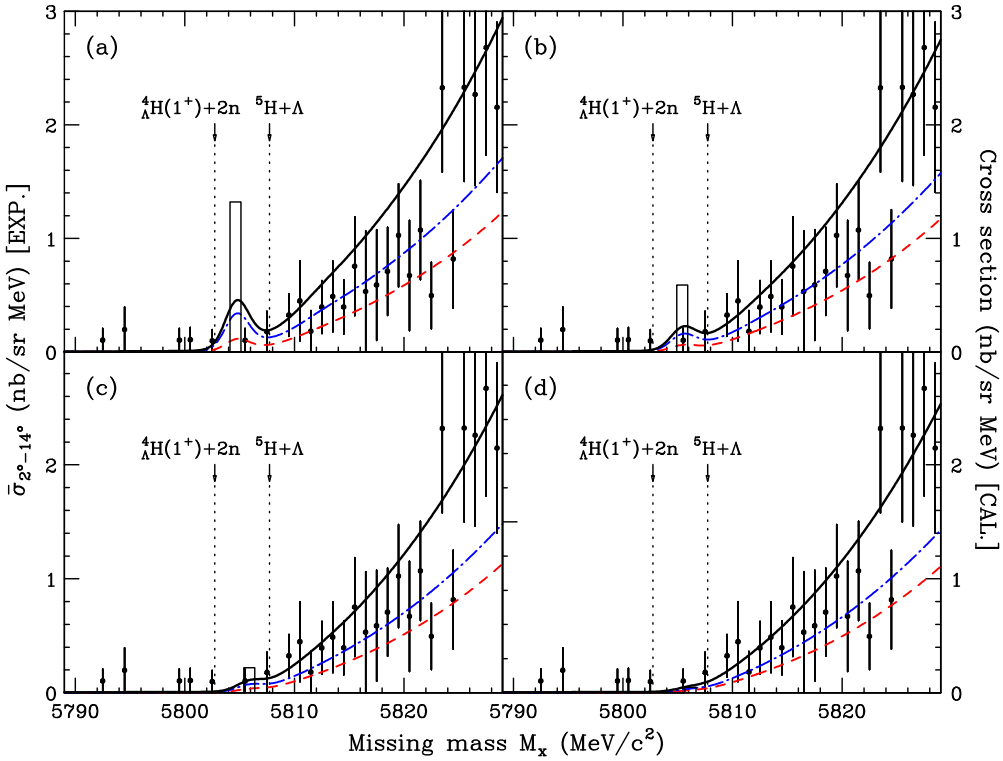

FIG. 6. Calculated missing mass spectra of the ^{6}Li(π^-, K^+) reactions near the Λ threshold at 1.2 GeV/c and $\theta_{\rm lab} = 7°$, with a detector resolution of 3.2 MeV FWHM. The $\Sigma\Lambda$ coupling strengths of $\tilde{v}^1_{\Sigma N,\Lambda N}$ = (a) −1800, (b) −1350, (c) −900, and (d) −450 MeV [$\tilde{v}^0_{\Sigma N,\Lambda N}$ = (a) 1000, (b) 750, (c) 500, and (d) 250 MeV] are used, together with $V_\Lambda = -19$ MeV for the Λ-^{5}H potential. Solid, dashed and dot-dashed curves denote contribution of total, p-hole, and s-hole spectra, respectively. The data are taken from Ref. [1]. The bins with a finite width of 1 MeV denote the cross sections for $^6_\Lambda$H(1$^+_{\rm exc.}$) which is located in particle decay channels.

strength and also the loosely resonant Λ state in the ^{5}H nuclear core. Although the Σ^--mixing probabilities for $^6_\Lambda$H are very small, the sensitivity of the spectrum below the ^{5}H + Λ threshold on $\tilde{v}^S_{\Sigma N,\Lambda N}$ indicates the possibility to extract the precise Σ^- components in wave functions for $^6_\Lambda$H in the nuclear (π^-, K^+) reactions. We confirm that the $\Sigma\Lambda$ coupling potential plays an essential role in the formation of the Λ hypernuclear state near the Λ threshold. Consequently, the calculated spectrum seems to be in good agreement with that of the ^{6}Li(π^-, K^+) data when we use the $\Sigma\Lambda$ coupling strengths of $\tilde{v}^1_{\Sigma N,\Lambda N} \simeq -900$ MeV and $\tilde{v}^0_{\Sigma N,\Lambda N} \simeq 500$ MeV, whose values correspond to those of the volume integrals for the D2′g potential [39].

C. V_Λ strengths

On the other hand, another important parameter V_Λ for the ^{5}H-Λ potential also affects the binding energies and the production cross sections for $^6_\Lambda$H(1$^+_{\rm exc.}$). The energy position of $^6_\Lambda$H(1$^+_{\rm exc.}$) is shifted downward by the attraction of V_Λ. We find that, when $\tilde{v}^1_{\Sigma N,\Lambda N} = -900$ MeV and $\tilde{v}^0_{\Sigma N,\Lambda N} = 500$ MeV, the binding energies are $B_\Lambda(^6_\Lambda{\rm H}) = 0.050$, 1.841, 3.726 and 5.493 MeV for $V_\Lambda = -11$, −19, −24, and −28 MeV, respectively, so that the Σ^--mixing probabilities amount to $P_{\Sigma^-} = 0.07\%$, 0.32%, 0.38%, and 0.40%. In Fig. 7, we show the dependence of the inclusive Λ spectrum for the $^6_\Lambda$H(1$^+_{\rm exc.}$) production on these values of V_Λ when $\tilde{v}^1_{\Sigma N,\Lambda N} = -900$ MeV and $\tilde{v}^0_{\Sigma N,\Lambda N} =$ 500 MeV. We show that the calculated spectrum for $^6_\Lambda$H(1$^+_{\rm exc.}$) is considerably changed by the value of V_Λ, where the integrated cross sections of $^6_\Lambda$H(1$^+_{\rm exc.}$) become $d\sigma/d\Omega = 0.04$, 0.22, 0.34

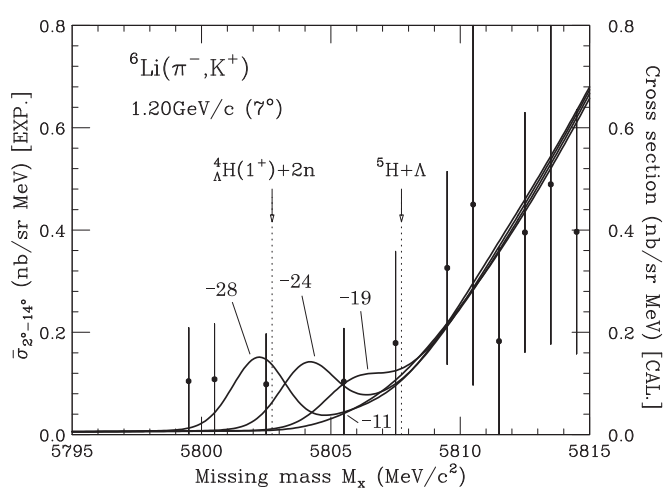

FIG. 7. Dependence of the calculated inclusive Λ spectrum in the ^{6}Li(π^-, K^+) reaction at $p_{\pi^-} = 1.2$ GeV/c (7°) on various strengths of V_Λ, together with the experimental data [1]. Solid curves denote the spectra by $V_\Lambda = -28$, −24, −19, and −11 MeV when $\tilde{v}^1_{\Sigma N,\Lambda N} = -900$ MeV and $\tilde{v}^0_{\Sigma N,\Lambda N} = 500$ MeV with a detector resolution of 3.2 MeV FWHM.

and 0.41 nb/sr for $V_\Lambda = -11$, -19, -24, and -28 MeV, respectively. The calculated spectra with $V_\Lambda = (-24)$–(-28) MeV seem to disagree with the data of no peak structure below the $^5\mathrm{H} + \Lambda$ threshold. This fact may indicate that the ^{5}H-Λ potential is quite shallow in comparison with the Λ-nucleus potentials which are well known as $V_\Lambda \simeq -28$ MeV in ordinary nuclei [30], and the neutron-rich nuclear core ^{5}H should be an unbound or broad resonant state.

D. V_Σ and W_Σ strengths

As discussed above, we recognize that the calculated spectrum is in good agreement with that of the $^6\mathrm{Li}(\pi^-, K^+)$ data when we use the $\Sigma\Lambda$ coupling strengths of $\tilde{v}^1_{\Sigma N,\Lambda N} \simeq -900$ MeV and $\tilde{v}^0_{\Sigma N,\Lambda N} \simeq 500$ MeV, together with $V_\Sigma \simeq (+20)$–$(+30)$ MeV and $W_\Sigma \simeq -20$ MeV for the ^{5}He-Σ^- potential [19]. The nature of the repulsive component in this potential is consistent with that in the Σ-nucleus potential obtained on heavier targets [17]. The calculated spectrum fully explains the data in the Σ^- and Λ QF regions by the one-step mechanism, $\pi^- p \to K^+\Sigma^-$ via Σ^- doorways caused by the $\Sigma^- p \leftrightarrow \Lambda n$ coupling.

E. $^5\mathrm{H}(1/2^+_{\mathrm{g.s}})$ resonant state

Current experiments have reported that the ^{5}H ground state is located at $E_r = 1.7 \pm 0.3$ MeV with $\Gamma = 1.9 \pm 0.4$ MeV above the $^3\mathrm{H} + 2n$ threshold [29], or at $E_r = 5.5 \pm 0.2$ MeV with $\Gamma = 5.4 \pm 0.6$ MeV [45]. The problem of whether the $^5\mathrm{H}(1/2^+_{\mathrm{g.s.}})$ ground state exists as a narrow resonant state with $E_r = 1.7$ MeV and $\Gamma = 1.9$ MeV may still be unsettled [22,28]. Several theoretical investigations [22,25] suggest the energy of the ^{5}H ground state with $E_r \simeq 1.6$–3.0 MeV, $\Gamma \simeq 1.5$–4.0 MeV in *tnn* three-body calculations [25] and $E_r \simeq 3.0$–4.5 MeV in the shell-model calculations with *spsd* space [26,27]. It is expected that the $\Sigma\Lambda$ coupling matrix elements work reasonably within the shell-model description. In the viewpoint of shell-model calculations, we assume that the $^5\mathrm{H}(1/2^+_{\mathrm{g.s.}})$ nuclear core is a resonant state with $E_r = 4.0$ MeV, rather than that with $E_r = 1.7$ MeV; if we have $E_r = 1.7$ MeV in the shell models, we would need to artificially add an extreme attraction to the ^{5}H system, e.g., by three-nucleon forces [10]. To see effects of the energy of the $^5\mathrm{H} + \Lambda$ threshold on $^6_\Lambda\mathrm{H}(1^+_{\mathrm{exc.}})$, we calculate the inclusive spectrum near the Λ threshold, changing the energy of the $^5\mathrm{H}(1/2^+_{\mathrm{g.s.}})$ resonant state. In Fig. 8, we show the dependence of the inclusive Λ spectrum for $^6_\Lambda\mathrm{H}(1^+_{\mathrm{exc.}})$ near the Λ threshold, using $E_r = 4.0$ MeV and 1.7 MeV which determine the position of the $^5\mathrm{H} + \Lambda$ threshold. We recognize that the shape of the calculated spectrum for $^6_\Lambda\mathrm{H}(1^+_{\mathrm{exc.}})$ is considerably changed by the value of E_r which depends on whether ^{5}H is a narrow resonant state. The structure of ^{5}H may influence the scenario of production of $^6_\Lambda$H at FINUDA [5]. Thus the spectrum near the Λ threshold provides the ability to study the structure of the ^{5}H core nucleus in detailed comparison with the precise data, as well as the structure of $^6_\Lambda\mathrm{H}(1^+_{\mathrm{exc.}})$.

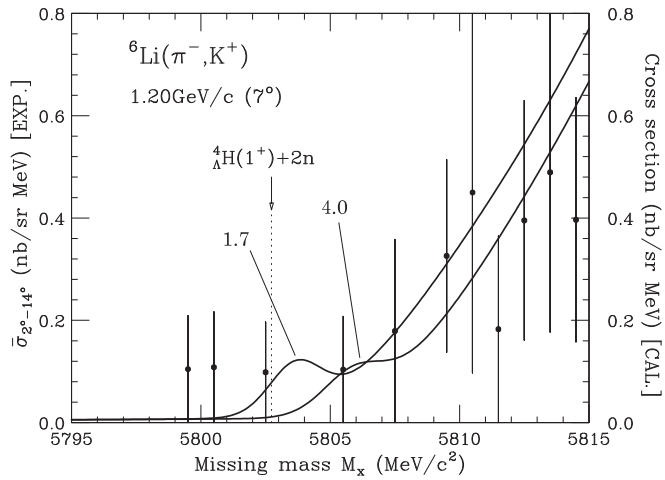

FIG. 8. Comparison between the calculated inclusive Λ spectrum of $E_r = 4.0$ MeV and that of $E_r = 1.7$ MeV for the energy of $^5\mathrm{H}(1/2^+_{\mathrm{g.s.}})$ in the $^6\mathrm{Li}(\pi^-, K^+)$ reaction at $p_{\pi^-} = 1.2$ GeV/c (7°). $V_\Lambda = -19$ MeV is used. See also the caption in Fig. 7.

F. Finite range

To clarify the one-step mechanism for production of the neutron-rich Λ hypernucleus, we obtained the $\Sigma\Lambda$ coupling potential constructed by the zero-range two-body interaction for simplicity, using the WS form for diagonal potentials in $^5\mathrm{H} + \Lambda$ and $^5\mathrm{He} + \Sigma^-$ channels. On the other hand, it is known that a finite range of the two-body interaction provides modified nuclear potentials [31]. To see effects of the finite range of the interaction, we have a Gaussian shape, $v^S_{\Sigma N,\Lambda N}(\boldsymbol{r}',\boldsymbol{r}) = v^S_{\Sigma N,\Lambda N}(\mathrm{FR}) \exp(-|\boldsymbol{r}' - \boldsymbol{r}|^2/\beta^2)$, where β is a range parameter. Here we choose $v^1_{\Sigma N,\Lambda N}(\mathrm{FR}) = -369.4$ MeV and $v^0_{\Sigma N,\Lambda N}(\mathrm{FR}) = 205.2$ MeV for $\beta = 0.8$ fm; these strength parameters correspond to a spin-averaged ΛN strength of $\bar{v}_{\Lambda N}(\mathrm{FR}) = -105.9$ MeV with $\beta = 0.8$ fm, which reproduce the Λ binding energies for light p-shell nuclei. In the folding potential model, we realize that the radial shape of the $\Sigma\Lambda$ coupling potential $U_X(r)$ is more smoothly behaved and the range of $U_X(r)$ becomes slightly extended. Thus we find that the Σ^--mixing probabilities for $^6_\Lambda\mathrm{H}(1^+_{\mathrm{exc.}})$ account for $P_{\Sigma^-}(s_\Sigma) = 0.13\%$ and $P_{\Sigma^-}(p_\Sigma) = 0.11\%$ in comparison with 0.13% and 0.17% shown in Table II. The integrated cross section for $^6_\Lambda\mathrm{H}(1^+_{\mathrm{exc.}})$ is $d\sigma/d\Omega = 0.17$ nb/sr and the (π^-, K^+) spectrum is not so modified. It seems that a value of $P_{\Sigma^-}(p_\Sigma)$ is relatively reduced whereas $P_{\Sigma^-}(s_\Sigma)$ is not changed. This modification may depend on nuclear structures of the ^{5}H and ^{5}He core states as well as properties of the two-body ΛN, ΣN and ΛN–ΣN effective interactions. Therefore, more investigation is needed to qualitatively clarify nuclear dynamics by sophisticated microscopic calculations.

G. Two-step processes of $\pi^- p \to K^0\Lambda$ followed by $K^0 p \to K^+ n$

Finally we discuss the integrated laboratory cross sections of $d\sigma/d\Omega$ for $^6_\Lambda\mathrm{H}(1^+_{\mathrm{exc.}})$ by the two-step mechanism, $\pi^- p \to K^0\Lambda$ followed by $K^0 p \to K^+ n$ or $\pi^- p \to \pi^0 n$ followed by $\pi^0 p \to K^+\Lambda$ in the DCX $^6\mathrm{Li}(\pi^-, K^+)$ reaction for production of the neutron-rich Λ hypernuclei [13]. We

roughly estimate the contribution of the two-step processes for $\pi^- p \to K^0 n$ followed by $K^0 p \to K^+\Lambda$, which are expected to be a main component, rather than those for $\pi^- p \to \pi^0 n$ followed by $\pi^0 p \to K^+\Lambda$. The sum of the cross sections by a harmonic oscillator model [46] for ^{6}Li targets at $p_{\pi^-} = 1.2$ GeV/c (0°) is given as

$$\sum_f \left(\frac{d\sigma_f^{(2)}}{d\Omega_L}\right)_{0^\circ} \approx \frac{2\pi\xi}{p_K^2}\left\langle\frac{1}{r^2}\right\rangle\left(\alpha\frac{d\sigma}{d\Omega_L}\right)_{0^\circ}^{\pi^- p\to K^0\Lambda} \times \left(\alpha\frac{d\sigma}{d\Omega_L}\right)_{0^\circ}^{K^0 p\to K^+ n} N_{\rm eff}^{pp}, \qquad (16)$$

where $\xi = 0.0370$ mb^{-1} is the factor integrated over angle $\theta_{\rm lab}^{(K^0)}$ for $\pi^- p \to K^0\Lambda$ with $-\theta_{\rm lab}^{(K^+)}$ for $K^0 p \to K^+ n$ to restore $\theta_{\rm lab} = 0^\circ$ in the angular distributions of the two elementary processes, $p_K \simeq 0.842$ GeV/c is the intermediate kaon momentum, and $\langle 1/r^2\rangle \simeq 0.0280$ mb^{-1} is the mean inverse-square radial separation of the proton pair. $N_{\rm eff}^{pp} \simeq 1$ is the effective number of proton pairs including the nuclear distortion effects. The elementary laboratory cross section $(\alpha d\sigma/d\Omega_L)_{0^\circ}$ is estimated to be ~0.35 mb/sr for $\pi^- p \to K^0\Lambda$ or ~1.96 mb/sr for $K^0 p \to K^+ n$, depending on the nuclear medium corrections. The results show $\sum_f (d\sigma_f^{(2)}/d\Omega_L)_{0^\circ} \simeq 1.4$–$1.9$ μb/sr for $\pi^- p \to K^0 n$ followed by $K^0 p \to K^+\Lambda$, and also 0.20–0.34 μb/sr for $\pi^- p \to \pi^0 n$ followed by $\pi^0 p \to K^+\Lambda$. Considering the large momentum transfer $q \simeq 360$ MeV/c in the (π^-, K^+) reactions, we expect that the production probabilities for loosely bound or resonant Λ states do not exceed 10^{-3}% in the quasielastic Λn production, so that the cross section of ${}^6_\Lambda$H in the two-step mechanism may be on the order of 10^{-2} nb/sr at $\theta_{\rm lab} = 7^\circ$. This result suggests that the one-step mechanism, $\pi^- p \to K^+\Sigma^-$ via Σ^- doorways caused by the $\Sigma^- p \leftrightarrow \Lambda n$ coupling is rather favored than the two-step mechanism.

V. SUMMARY AND CONCLUSION

We studied phenomenologically the production of a neutron-rich hypernucleus ${}^6_\Lambda$H in the ^{6}Li(π^-, K^+) reaction at 1.2 GeV/c, considering the DWIA in the one-step mechanism, $\pi^- p \to K^+\Sigma^-$ via Σ^- doorways caused by $\Sigma^- p \leftrightarrow \Lambda n$ coupling. We evaluated the production cross section of ${}^6_\Lambda$H$(1^+_{\rm exc.})$ by using the coupled $({}^5$H-$\Lambda) + ({}^5$He-$\Sigma^-)$ model with a spreading potential and compared it with the data of the missing mass spectrum at the J-PARC E10 experiment. The results are summarized as follows:

(i) The Σ^--mixing probabilities in ${}^6_\Lambda$H$(1^+_{\rm exc.})$ are $P_{\Sigma^-} \lesssim 0.2\%$ both for s_Σ state and for p_Σ state in order to reproduce no significant peak in the Λ production data, so that the cross section of ${}^6_\Lambda$H is less than on the order of 0.4 nb/sr.

(ii) The shape and magnitude of the near-Λ-threshold spectrum significantly depend on the $\Sigma\Lambda$ coupling and Λ potentials.

(iii) The cross section of ${}^6_\Lambda$H$(1^+_{\rm exc.})$ is also sensitive to the structure of the ^{5}H core nucleus independent of whether the ^{5}H$(1/2^+_{\rm g.s.})$ ground state exists as a resonant state bound with a narrow width.

(iv) The one-step mechanism via Σ^- doorways seems to be rather favored over the two-step mechanism because the cross section of ${}^6_\Lambda$H in the two-step mechanism may be on the order of 10^{-2} nb/sr at $\theta_{\rm lab} = 7^\circ$ by the harmonic-oscillator model.

In conclusion, the calculated spectrum of the ${}^6_\Lambda$H hypernucleus by the one-step mechanism via Σ^- doorways can evaluate the near-Λ-threshold data of the DCX ^{6}Li(π^-, K^+) reaction at 1.20 GeV/c. The result shows that the Σ^--mixing probabilities in ${}^6_\Lambda$H$(1^+_{\rm exc.})$ are $P_{\Sigma^-} \lesssim 0.2\%$ both for s_Σ state and for p_Σ state in order to explain no significant peak in the Λ production spectrum obtained at the J-PARC E10 experiment. The sensitivity to the potential parameters implies that the nuclear (π^-, K^+) reactions with much less background experimentally provide the high ability to study precise wave functions for Λ, Σ^- and the ^{5}H nuclear core in the neutron-rich Λ hypernucleus. Systematic analysis based on microscopic calculations is required for the extended J-PARC E10 experiment [47]. This investigation is in progress.

ACKNOWLEDGMENTS

The authors would like to thank Dr. R. Honda, Professor A. Sakaguchi, Professor H. Tamura, Dr. M. Ukai, and Professor T. Fukuda for many valuable discussions. This work was supported by JSPS KAKENHI Grants No. JP24105008, No. JP25400278, and No. JP16K05363.

[1] H. Sugimura *et al.* (J-PARC E10 Collaboration), Phys. Lett. B **729**, 39 (2014).
[2] R. Honda, Ph.D. thesis, Tohoku University, 2014 (unpublished).
[3] R. H. Dalitz and R. Levi-Setti, Nuovo Cimento **30**, 489 (1963).
[4] L. Majling, Nucl. Phys. A **585**, 211 (1995).
[5] M. Agnello *et al.* (FINUDA Collaboration), Phys. Rev. Lett. **108**, 042501 (2012).
[6] Y. Akaishi and Khin Swe Myint, AIP Conf. Proc. **1011**, 277 (2008).
[7] Y. Akaishi, T. Harada, S. Shinmura, and Khin Swe Myint, Phys. Rev. Lett. **84**, 3539 (2000).
[8] Khin Swe Myint, T. Harada, S. Shinmura, and Y. Akaishi, Few-Body Syst. Suppl. **12**, 383 (2000); S. Shinmura, Khin Swe Myint, T. Harada, and Y. Akaishi, J. Phys. G **28**, 1 (2002).
[9] A. Gal and D. J. Millener, Phys. Lett. B **725**, 445 (2013).
[10] E. Hiyama *et al.*, Nucl. Phys. A **908**, 29 (2013).
[11] P. K. Saha *et al.*, Phys. Rev. C **70**, 044613 (2004).
[12] T. Yu. Tretyakova and D. E. Lanskoy, Phys. At. Nucl. **66**, 1651 (2003); Nucl. Phys. A **691**, 51 (2001).
[13] T. Harada, A. Umeya, and Y. Hirabayashi, Phys. Rev. C **79**, 014603 (2009).

[14] T. Harada, Phys. Rev. Lett. **81**, 5287 (1998); Nucl. Phys. A **672**, 181 (2000).
[15] J. Hüfner, S. Y. Lee, and H. A. Weidenmüller, Nucl. Phys. A **234**, 429 (1974).
[16] O. Morimatsu and K. Yazaki, Prog. Part. Nucl. Phys. **33**, 679 (1994), and references therein.
[17] T. Harada and Y. Hirabayashi, Nucl. Phys. A **759**, 143 (2005); **767**, 206 (2006).
[18] Y. Fujiwara, H. Horiuchi, K. Ikeda, M. Kamimura, K. Katō, Y. Suzuki, E. Uegaki, Prog. Theor. Phys. Suppl. **68**, 29 (1980); H. Furutani, H. Kanada, T. Kaneko, S. Nagata, H. Nishioka, S. Okabe, S. Saito, T. Sakuda, and M. Seya, *ibid.* **68**, 193 (1980).
[19] T. Harada, R. Honda, and Y. Hirabayashi (unpublished).
[20] A. Bohr and M. Mottelson, *Nuclear Structure* (Benjemin, New York, 1969), Vol.1, p. 238.
[21] H. Tyeén *et al.*, Nucl. Phys. **79**, 321 (1966); G. Jacob and Th. A. Maris, Rev. Mod. Phys. **45**, 6 (1973).
[22] D. R. Tilley *et al.*, Nucl. Phys. A **708**, 3 (2002).
[23] H. de Vries, C. W. de Jager, and C. de Vries, At. Data Nucl. Data Tables **36**, 495 (1987).
[24] Y. Sakuragi, M. Yahiro, and M. Kamimura, Prog. Theor. Phys. **70**, 1047 (1983).
[25] R. de Diego *et al.*, Nucl. Phys. A **786**, 71 (2007).
[26] S. Cohen and D. Kurath, Nucl. Phys. A **101**, 1 (1967); D. J. Millener and D. Kurath, *ibid.* **255**, 315 (1975).
[27] J. J. Bevelacqua, Nucl. Phys. A **357**, 126 (1981).
[28] J. Tanaka *et al.*, Determination of precise mass and width of ^{5}H, Proposal for E428 experiment at RCNP (2014); http://www.rcnp.osaka-u.ac.jp/Divisions/plan/b-pac/ex_appro/index.html.
[29] A. A. Korsheninnikov *et al.*, Phys. Rev. Lett. **87**, 092501 (2001); M. S. Golovkov *et al.*, Phys. Lett. B **566**, 70 (2003).
[30] D. J. Millener, C. B. Dover, and A. Gal, Phys. Rev. C **38**, 2700 (1988).
[31] N. K. Glendenning, *Direct Nuclear Reactions* (Academic Press, New York, 1983), p.144.
[32] T. Harada, Y. Hirabayashi, and A. Umeya, Phys. Lett. B **690**, 363 (2010).
[33] N. Auerbach, Phys. Rev. C **35**, 1798 (1987).
[34] A. E. L. Dieperink and T. de Forest, Phys. Rev. C **10**, 543 (1974).
[35] M. M. Nagels, T. A. Rijken, and J. J. de Swart, Phys. Rev. D **15**, 2547 (1977).
[36] P. M. M. Maessen, T. A. Rijken, and J. J. de Swart, Phys. Rev. C **40**, 2226 (1989).
[37] Y. Yamamoto *et al.*, Prog. Theor. Phys. Suppl. **117**, 361 (1994).
[38] Y. Yamamoto, T. Motoba, and T. A. Rijken, Prog. Theor. Phys. Suppl. **185**, 72 (2010).
[39] T. Harada and Y. Hirabayashi, Phys. Rev. C **89**, 054603 (2014).
[40] C. B. Dover, L. Ludeking, and G. E. Walker, Phys. Rev. C **22**, 2073 (1980).
[41] H. Kamano, S. X. Nakamura, T. -S. H. Lee, and T. Sato, Phys. Rev. C **88**, 035209 (2013); S. X. Nakamura (private communication).
[42] H. Nemura, Y. Akaishi, and Y. Suzuki, Phys. Rev. Lett. **89**, 142504 (2002).
[43] A. Umeya and T. Harada, Phys. Rev. C **79**, 024315 (2009); **83**, 034310 (2011).
[44] D. J. Millener, Springer Lec. Notes Phys. **724**, 31 (2007); Nucl. Phys. A **804**, 84 (2008).
[45] Yu. B. Gurov *et al.*, Eur. Phys. J. A **24**, 231 (2005).
[46] R. E. Chrien, C. B. Dover, and A. Gal, Czech. J. Phys. B **42**, 1089 (1992).
[47] A. Sakaguchi *et al.*, Production of Neutron-Rich Λ-Hypernuclei with the Double Charge-Exchange Reactions, Proposal for Nuclear and Particle Physics experiments at the J-PARC (2007); http://j-parc.jp/NuclPart/Proposal_e.html